The Effects of Gas-Phase and In-Depth Radiation Absorption on Ignition and Steady Burning Rate of PMMA

J. E. J. Staggs
Energy Research Institute
University of Leeds
Leeds LS2 9JT
United Kingdom

Keywords: PMMA; in-depth absorption; ignition; pyrolysis.

Abstract

Although well studied, there are still interesting features about the ignition and steady burning rate behaviour of PMMA when heated by thermal radiation. In this contribution, the dependence on external heat flux of ignition delay time and steady mass flux of PMMA are investigated numerically. Ignition is modelled by the critical mass flux criterion. The heat transfer model includes effects of heat lost by out gassing, change of volume during degradation and absorption of radiation in both condensed and gaseous phases. Model results are compared to experimental data for both ignition delay time and quasi-steady mass flux across a range of heat fluxes from 20 to 210 kWm^{-2} and the importance of both gas-phase and condensed-phase radiation absorption effects are discussed.

Nomenclature

Roman Symbols

c Specific heat capacity / $Jkg^{-1}K^{-1}$

D Thermal diffusivity / m^2s^{-1}

h Convection heat transfer coefficient / $Wm^{-2}K^{-1}$

H Reaction heat / Jkg^{-1}

J Natural log of pre-exponential factor

k	Arrhenius reaction rate / s^{-1}
l	Sample thickness / m
$\dot{m}''$	Mass flux / $kgs^{-1}m^{-2}$
$\dot{m}'''$	Mass production rate per unit volume / $kgs^{-1}m^{-3}$
$\dot{q}''$	Heat flux / Wm^{-2}
s	Location of exposed surface of sample / m
t	Time / s
T	Temperature / K
y	Distance into sample normal to exposed surface / m
z	Distance above sample normal to exposed surface / m

Greek Symbols

α	Absorptivity
δ	Characteristic thermal penetration depth / m
ε	Emissivity
κ	Absorption coefficient
λ	Thermal conductivity / $Wm^{-1}K^{-1}$
μ	Gas-phase absorption parameter / sm^2kg^{-1}
ρ	Density / kgm^{-3}
σ	Stefan-Boltzmann constant / $Wm^{-2}K^{-4}$

Important Subscripts

a	Ambient conditions
ig	A quantity at ignition
0	A quantity at the initial location of the exposed surface (y = 0)
s	A quantity at the moving exposed surface (y = s)
∞	A steady-state value

1. Introduction

For high heating rates, heat loss mechanisms are insignificant for short exposures and so one might expect that ignition behaviour of simple solids under such conditions would be dominated by external heat flux. If the often-used engineering

simplification of ignition at a critical surface temperature is adopted, it follows that the reciprocal of the square root of ignition time should be proportional to external heat flux. Interestingly, this turns out not to be the case [1] - [5]. After a thorough analysis of a one-dimensional mathematical model for ignition (including an alternative criterion for ignition) Bal & Rein [5] concluded that the observed variation of ignition time from the inverse square root correlation at high external heat flux could not be explained by:

- Taking heat losses into account at the exposed surface.
- Using a critical mass flux rather than a critical surface temperature ignition criterion.
- Using a more detailed reaction scheme for condensed phase degradation.
- Incorporation of temperature dependent thermal properties.

They went on to demonstrate that the deviation of ignition delay time from the inverse square root correlation could be explained by in-depth absorption of radiation in the condensed phase.

Measurements of the transmissivity of black PMMA (Polycast) [4] suggest that the absorption coefficient κ is approximately $960 m^{-1}$, indicating a characteristic absorption depth of ~1mm. If the external heat flux is $\dot{q}''$ at the exposed surface, T is temperature and λ is thermal conductivity then ignoring in-depth absorption, the characteristic thermal penetration depth assuming conduction heat transfer is $\delta \sim \lambda \Delta T / \dot{q}''$, where ΔT is a physically significant temperature interval. For ignition it is sensible to take ΔT as the characteristic kinetic temperature range [6], which corresponds approximately to the temperature range over which the material pyrolyses at constant heating rate. Thus it seems reasonable that in-depth absorption of radiation becomes important when $\kappa\delta << 1$, i.e. when $\dot{q}'' >> \kappa\lambda\Delta T$. For PMMA with κ as above, λ = 0.2 $Wm^{-1}K^{-1}$ and ΔT ~ 150 K (see Figure 4 below), $\kappa\lambda\Delta T$ is approximately 30 kWm^{-2} and so it is likely that in-depth absorption should be accounted for at high radiation heat flux.

In-depth absorption of radiation in the condensed phase is only part of the problem, however. Kashiwagi's observations of ignition of PMMA by CO_2 laser [1] show that there is significant absorption of radiation by gaseous MMA in the plume above the degrading sample and the role of gas-phase absorption in ignition and steady burning rate is unclear. Measurements of quasi-steady mass flux (the approximately steady mass loss rate per unit surface area due to out-gassing of volatiles for an initially thick sample, also referred to as "burning rate") as external heat flux is varied indicate a nonlinear trend at high heat flux [2] - [4]. This is unexpected from simple ablation theory, which predicts that steady mass flux should be proportional to the ratio of net heat flux at the exposed surface to heat of gasification [7] - [11]. If radiation absorption in the condensed phase provides an explanation for the observed variation of ignition delay time, then does it also account for the observed trend in mass flux?

In this paper, a mathematical model of ignition and pyrolysis of PMMA is carefully investigated. Naturally in-depth absorption of radiation is included, but other features not considered in Bal & Rein's model [5] are also included such as heat lost by out-gassing and change of volume during degradation. Change of volume occurs as the sample pyrolyses. It is unlikely that this will have much effect on ignition behaviour, especially at high heat flux, but an early paper by the author [12] demonstrates that it can have a significant effect on mass flux at moderate heat flux. Bal & Rein accounted for gas-phase absorption using the device of a gas-phase absorption coefficient, assuming that a constant fraction of the incident radiation is absorbed by the pyrolyzate above the exposed surface. In this approach a more involved model of gas-phase absorption is developed, where the amount of absorption depends on the mass flux of pyrolyzate. We begin with a brief discussion of the expected, order of magnitude, effect of condensed phase absorption on ignition. We then go on to consider a more detailed model of pyrolysis and ignition together with a simplified model for gas phase absorption of radiation. Where possible parameter values for the model are chosen based on either literature values or experimental data and, prior to the main analysis, results are compared with experimental cone calorimeter data for mass flux. The roles of condensed- and gas-phase absorption of radiation in ignition and steady burning rate are then investigated numerically.

2. Ignition at a Critical Temperature

2.1 The General Problem

The simplest possible model of ignition is the critical surface temperature approximation, where ignition is assumed to occur as soon as the exposed surface reaches a characteristic temperature T_{ig}. Bal & Rein [5] concluded that ignition behaviour at high heat flux was not greatly affected by the choice of ignition criterion (critical temperature or critical mass flux) and so for convenience we shall adopt the simpler approach for this order of magnitude analysis. Coincident with this approximation of ignition is the additional assumption that the solid remains inert for temperatures below T_{ig}.

When in-depth absorption of radiation occurs in a 1-D translucent solid, the total heat flux $\dot{q}''$ consists of two components: $\dot{q}'' = -\lambda \partial T / \partial y + \dot{q}''_R$. Here the first part is conducted heat flux, where y is distance below the exposed surface, and $\dot{q}''_R$ is transmitted radiation flux. Thus for an inert solid with constant thermal properties, conservation of energy implies that

$$\rho c \frac{\partial T}{\partial t} = \frac{\partial}{\partial y}\left(\lambda \frac{\partial T}{\partial y} - \dot{q}''_R \right). \qquad (1)$$

Here ρ is density and c is specific heat capacity. Usually, the in-depth radiation term is modelled by Beer's law: $\dot{q}''_R = (1-\alpha_R)\dot{q}''_0 \exp(-\kappa y)$. Here κ is the absorption coefficient already defined above.

At the exposed surface ($y = 0$) of the solid there are three possibilities for the fate of incident radiation: it can be absorbed, reflected or transmitted. For simplicity it shall be assumed that there is no reflected radiation. The unexposed surface ($y = l$) is assumed to be well insulated and opaque, so the net heat flux there is zero. Under these conditions, the boundary conditions are

$$-\lambda\frac{\partial T}{\partial y}=\alpha_R\dot{q}_0''+h\left(T_a-T\right)+\varepsilon\sigma\left(T_a^4-T^4\right)\ \text{at}\ \ y=0, \tag{2}$$

$$-\lambda\frac{\partial T}{\partial y}+\dot{q}_R''=0\ \text{at}\ \ y=l. \tag{3}$$

Here α_R is absorptivity, $\dot{q}_0''$ is incident radiation, h is the convection heat transfer coefficient, T_a is ambient temperature, ε is emissivity and σ is the Stefan-Boltzmann constant. When Kirchoff's law applies, the emissivity and absorptivity are equal, however there is no guarantee that this is always true.

Applying the boundary conditions at the exposed and unexposed surfaces, it follows that the steady-state temperature distribution $T_\infty(y)$ is given by

$$T_\infty(y)=T_0+\frac{1}{\lambda}\int_0^y\dot{q}_R''\,dy, \tag{4}$$

where T_0 (the temperature at y = 0) satisfies $\dot{q}_0''+h\left(T_a-T_0\right)+\varepsilon\sigma\left(T_a^4-T_0^4\right)=0$.

The solution of the transient inert problem presents no particular difficulties. Delichatsios and Zhang present an approximate solution in [13]. However for what follows below it is worth considering the high heat flux limit in some detail.

2.2 High Heat Flux Limit

Here we note that if the external heat flux is sufficiently high, so that $\alpha_R\dot{q}_0''>>h\left(T_{ig}-T_a\right)+\varepsilon\sigma\left(T_{ig}^4-T_a^4\right)$, where T_{ig} is the temperature at ignition, then heat losses are negligible[1] up to ignition. This is illustrated in Figure 1, where the regions

[1] Note that this is equivalent to the external heat flux being very much greater than the critical heat flux (see next section).

above the curves correspond to high external heat fluxes for different values of the radiation parameter $\varepsilon\sigma T_{ig}^3 / h$.

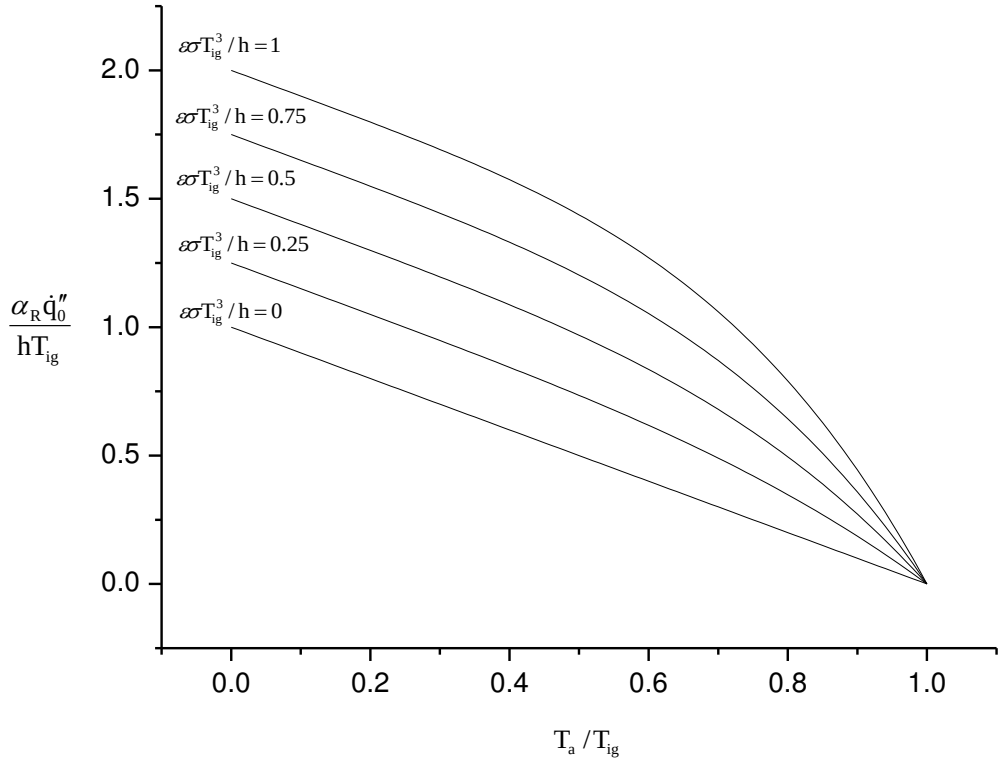

Figure 1. High heat flux limits.

When this is the case, setting

$$T = T_1 + T_a + \frac{\dot{q}_0''}{l\rho c} t - \frac{\dot{q}_0'' y}{\lambda}\left(1 - \frac{y}{2l}\right) + \frac{1}{\lambda}\int_0^y \dot{q}_R'' \, dy, \qquad (5)$$

and substituting this expression into (1) it follows that T_1 must satisfy the standard diffusion equation $\partial T_1 / \partial t = D\partial^2 T_1 / \partial y^2$, where $D = \lambda / (\rho c)$ is the thermal diffusivity. Furthermore, application of the boundary conditions (2) and (3) without surface heat losses implies that $\partial T_1 / \partial y = 0$ at both bounding surfaces. Since the initial temperature is assumed to be ambient throughout, the initial temperature distribution for T_1 must be

$$T_1(0, y) = \frac{\dot{q}''_0 y}{\lambda}\left(1 - \frac{y}{2l}\right) - \frac{1}{\lambda}\int_0^y \dot{q}''_R \, dy . \tag{6}$$

If Beer's law is assumed, it is immediately apparent from Eqn. (5) that for ignition at a critical temperature T_{ig}, the ignition time t_{ig} will be of the form

$$t_{ig} = \frac{l^2}{D} f\left(\frac{T_{ig}}{T_a}, \frac{l\dot{q}''_0}{\lambda T_a}, \alpha_R, \kappa l\right). \tag{7}$$

Alternatively, in the high heat flux limit (HHFL) for a thick solid, the temperature profile may be approximated by

$$T \sim \begin{cases} T_0(t) + (T_a - T_0(t))y/\delta(t), 0 \le y \le \delta(t), \\ T_a, \; y > \delta(t), \end{cases} \tag{8}$$

where $T_0(t)$ is again the temperature at the exposed surface y = 0 and $\delta(t)$ is the thermal penetration depth (now a function of time). Integrating the temperature equation (1) over the thermal penetration depth, we find that $\rho c \int_0^\delta \partial T/\partial t \, dy = \dot{q}''_0\{1 - (1-\alpha_R)e^{-\kappa\delta}\}$. Now using the facts that $\frac{d}{dt}\int_0^\delta T dy = T_a \, d\delta/dt + \int_0^\delta \partial T/\partial t \, dy$, $\int_0^\delta T dy \sim \frac{\delta}{2}(T_0 + T_a)$ and $d/dt = d\delta/dt \, d/d\delta$ it follows that

$$\frac{\rho c}{2}\frac{d\delta}{dt}\left\{T_0 - T_a + \delta\frac{dT_s}{d\delta}\right\} \sim \dot{q}''_0\{1 - (1-\alpha_R)e^{-\kappa\delta}\}. \tag{9}$$

The boundary condition on the exposed surface means that $T_0 - T_a = \alpha_R \dot{q}''_0 \delta/\lambda$ and so when the external heat flux is sufficiently high, such that $\dot{q}''_0 >> \lambda\kappa(T_{ig} - T_a)/\alpha_R$, it follows that $\kappa\delta$ will always be small. Therefore $d(\delta^2)/dt \sim 2D$, in the HHFL and so $\delta \sim \sqrt{2Dt}$. Hence ignition time t_{ig} and ignition temperature will be approximately

related by $T_{ig} \sim T_a + \alpha_R \dot{q}''_0 \sqrt{2Dt_{ig}} / \lambda$ and consequently in terms of the parameter groupings given in Eqn. (7) above,

$$t_{ig} \sim \frac{l^2}{D} . \frac{1}{2\alpha_R^2} . \left(\frac{T_{ig}}{T_a} - 1 \right)^2 . \left(\frac{\lambda T_a}{l \dot{q}''_0} \right)^2 . \tag{10}$$

In particular, it follows that

$$\frac{1}{\sqrt{t_{ig}}} \sim \frac{\alpha_R \dot{q}''_0 \sqrt{2D}}{\lambda (T_{ig} - T_a)} \tag{11}$$

and so we see that $1/\sqrt{t_{ig}}$ will reduce in direct proportion to α_R.

3. Ignition at a Critical Mass Flux: Reactive Solid

3.1 Energy Equation

Consider for simplicity a solid that on heating undergoes a single-step first-order degradation reaction of the form $dm/dt = -k(T)m$, where m is the ratio of sample mass to initial mass, $k(T) = \exp(J - T_A/T)$, J is the natural logarithm of the pre-exponential factor and T_A is the activation temperature. Bal & Rein [5] showed that ignition behaviour was not greatly affected by inclusion of a more sophisticated pyrolysis model, so only this simple first-order single-step approach will be investigated. Also, as above, heat transfer in one direction only (normal to the exposed surface) is modelled. Now consider a thick sample of solid where temperature gradients are not negligible. As the solid is heated gas is generated, which we assume escapes as soon as it forms (so that the local density ρ remains constant). This implies that there will be a reduction in sample volume as gasification proceeds (see Figure 2).

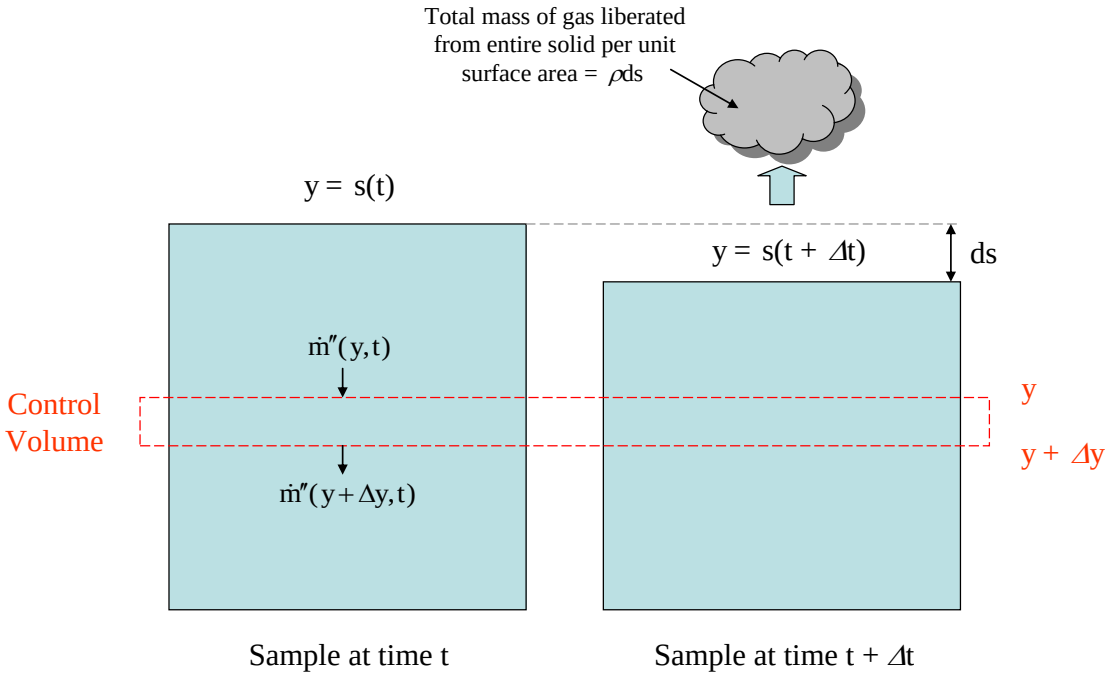

Figure 2. Definition of control volume.

The degradation reaction implies that the generation rate of gas per unit sample volume will be given by $\dot{m}_g''' = \rho k$. Let the location of the exposed surface be given by $y = s(t)$, where $s(0) = 0$. Now consider a control volume fixed in space, located between y and $y + \Delta y$, and let $\dot{m}''(y,t)$ denote the mass flux of solid that flows past point y at time t due to the reduction of volume.

Conservation of mass then implies that $\partial \dot{m}'' / \partial y = -\dot{m}_g'''$ and integrating this, we find that the local mass flux is given by $\dot{m}'' = \rho \int_y^l k dy$. Since the remaining solid mass per unit area is ρs, it follows that the location of the exposed surface will be given by the solution of the integro-differential equation

$$\frac{ds}{dt} = \int_s^l k dy, \; s(0) = 0. \tag{12}$$

Applying similar considerations to conservation of energy, it is possible to show that

$$\frac{\partial(\rho cT)}{\partial t} = -\frac{\partial(\dot{m}'' cT + \dot{q}'')}{\partial y} - \dot{m}_g'''(c_g T + H_g), \tag{13}$$

where, as above, the total heat flux $\dot{q}'' = -\lambda \partial T / \partial y + \dot{q}_R''$, H_g is the heat of the gasification reaction and $\dot{m}_g''' c_g T$ is the rate of outflow of heat per unit sample volume due to out-gassing, c_g being the specific heat capacity of the gas.

Using the expressions for $\dot{m}''$ and $\dot{m}_g'''$, the energy equation may be rewritten in more convenient form

$$\rho c \frac{\partial T}{\partial t} = -\rho c \frac{\partial T}{\partial y} \int_y^l k dy - \rho k \left[(c_g - c) T + H_g \right] + \frac{\partial}{\partial y} \left(\lambda \frac{\partial T}{\partial y} - \dot{q}_R'' \right). \tag{14}$$

Note that this equation must be solved throughout the volume of remaining solid $s(t) \le y \le l$.

3.2 Gas-Phase Attenuation of Incident Radiation

It is possible that radiation incident on the exposed surface may be attenuated by gas-phase absorption above the sample. Beaulieu [2], [3], was unable to estimate attenuation for a pyrolysing PMMA sample but instead used a propylene burner with an embedded heat flux gauge. She first measured the heat flux from the propylene flame only and then varied the output from the apparatus' external source and noted the new heat flux readings. She concluded that there was no attenuation by either the flame or the propylene gas. Earlier, Kashiwagi [1] conducted an elegant series of experiments on PMMA (and red oak) using a CO_2 laser as the radiation source. In his experiments, a small hole was cut in the samples and a heat flux gauge was placed directly beneath them so that he could measure attenuation through the pyrolyzate prior to ignition. He concluded that there was significant attenuation prior to ignition and that the ratio of incident heat flux to initial heat flux, i.e. 1 - attenuation, decreased approximately exponentially with time. Note that there is no contradiction

between these observations: Kashiwagi measured attenuation of the radiation by gaseous MMA and Beaulieu measured combined attenuation by propylene and a flame. There is no reason why these effects should be the same.

To estimate the effect of gas-phase attenuation, consider a column of pyrolyzate above the sample surface being advected upwards with speed v. In an instrument such as an oxygen consumption calorimeter, the mass flow rate of air is always much greater than mass flow rate of pyrolyzate, so to leading order we may assume that v is constant. Furthermore, consider a layer at height z above the sample surface at time t. The layer has taken time z/v to reach height z, and so the mass flux of pyrolyzate at the sample surface when the layer first formed was $\dot{m}''_g(t - z/v)$. Assuming there to be no mixing between layers in the column, in time step Δt it follows that the thickness of the layer will be $\Delta z = v\Delta t$ and the mass of pyrolyzate in the layer will be $\Delta m_p = A_t \dot{m}''_g(t - z/v)\Delta t$, where A_t is the cross-sectional area of the column. It is reasonable to suppose that attenuation of radiation through the layer will be directly proportional to the mass of pyrolyzate in the layer, since each particle has the potential to absorb radiation. In other words, we would expect that $(\dot{q}''_i(z,t) - \dot{q}''_i(z - \Delta z, t))/\dot{q}''_i(z,t) \propto \dot{m}''_g(t - z/v)\Delta t$, where $\dot{q}''_i(z,t)$ is the magnitude of radiation at height z and time t. It therefore follows that $\dot{q}''_i(z,t)$ satisfies

$$\frac{\partial \dot{q}''_i}{\partial z} = \frac{\eta}{v}\dot{q}''_i \dot{m}''_g(t - z/v), \tag{15}$$

where η is a constant of proportionality with dimensions m^2kg^{-1} that will depend on the absorbing properties of the pyrolyzate. Now, if the height of the column of pyrolyzate is z_{max} and the radiation at $z = z_{max}$ has magnitude $\dot{q}''_{ext}$, then the magnitude at the sample surface will be $\dot{q}''_s$, where

$$\dot{q}''_s = \dot{q}''_{ext} \exp\left(-\eta \int_0^{z_{max}/v} \dot{m}''_g(t - \tau)\mathrm{d}\tau \right). \tag{16}$$

Physically z_{max}/v is the time taken for the pyrolyzate to advect through the column and if this is small compared to the timescale on which out-gassing from the sample occurs, then

$$\dot{q}_s'' \approx \dot{q}_{ext}'' \exp\left(-\mu \dot{m}_g''(t)\right), \tag{17}$$

where $\mu = z_{max}\eta/v$ is an alternative constant with dimensions of sm^2kg^{-1}, which we shall refer to as the gas-phase absorption parameter. Physically, if one were able to measure the radiation flux at the exposed surface during pyrolysis, then μ would correspond to the gradient of the graph of $\ln(\dot{q}_{ext}''/\dot{q}_s'')$ plotted against the mass flux of escaping pyrolyzate.

It must be appreciated that the model set out above will be a gross oversimplification of the actual physical situation and serves only as a first-order approximation to quantify the effect of gas phase absorption. The flow field above the sample surface during out-gassing of volatile species will be complex and it is likely that this will have a large effect of the local density of pyrolyzate and hence attenuation. Furthermore, it should be noted that the nature of the experimental setup, including its physical dimensions, the wavelength of incident radiation and the total flow rate of gases, will also affect the value of μ.

3.3 Post Ignition Behaviour and Numerical Solution

In order to model post-ignition behaviour, an ignition criterion is required together with an additional term in the boundary condition at the exposed surface to account for heat flux from a flame. Here the device of critical mass flux [14] is used to determine ignition and following earlier observations [9], [10] it is assumed that the heat flux from a flame is constant. From the discussion above, we take

$$-\lambda \frac{\partial T}{\partial y} = \alpha_R \dot{q}_{ext}'' \exp\left(-\mu \dot{m}_g''(t)\right) + h(T_a - T) + \varepsilon\sigma\left(T_a^4 - T^4\right). \tag{18}$$

Here

$$\dot{q}''_{ext} = \begin{cases} \dot{q}''_0, \ \dot{m}''_g < \dot{m}''_{ign}, \\ \dot{q}''_0 + \dot{q}''_f, \ \dot{m}''_g \geq \dot{m}''_{ign}, \end{cases} \tag{19}$$

at the exposed surface, where $\dot{m}''_{ign}$ is the critical mass flux at ignition and $\dot{q}''_f$ is the flame heat flux.

We shall assume that Beer's law applies and so the in-depth radiation flux is now $\dot{q}''_R = (1-\alpha_R)\dot{q}''_{ext} \exp[-\kappa(y-s)]$.

Due to the nonlinearity of the temperature equation, recourse to numerical methods is inevitable. The method adopted here is a fully-implicit finite difference scheme with a non-uniform grid. In the numerical solution, the node density is greatest at the exposed surface so that temperature variation and the in-depth radiation term $\dot{q}''_R$ are adequately resolved[2]. The node density used in the calculations is shown in Figure 3.

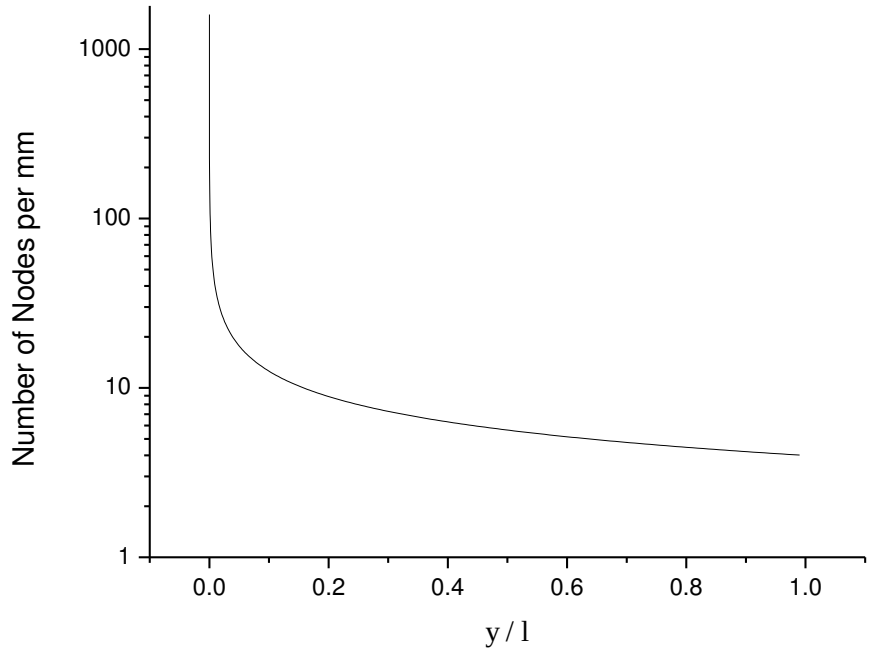

Figure 3. Node density (in number of nodes per mm) used in numerical calculations.

[2] The in-depth radiation flux at the exposed surface varies on a length scale of $1/\kappa$, so the node spacing Δy must be sufficiently small so that $\Delta y << 1/\kappa$, or equivalently the node density $1/\Delta y >> \kappa$.

4. Parameter Values

For convenience it will be assumed that Kirchoff's law is valid, i.e. $\varepsilon = \alpha_R$. The model parameters used in the numerical simulations, with the exception of the gas-phase absorption parameter, are given in Table 1 and are justified below.

Parameter	Symbol	Value
Ambient temperature	T_a	298 K
In-depth radiation length scale	$1/\kappa$	1 mm
Critical mass flux for ignition	$\dot{m}''_{ign}$	2.5 $gs^{-1}m^{-2}$
Convection heat transfer coefficient	h	25 $Wm^{-2}K^{-1}$
Absorptivity	α_R	0.56
Flame heat flux	$\dot{q}''_f$	23 kWm^{-2}
Thermal conductivity	λ	0.2 $Wm^{-1}K^{-1}$
Specific heat capacity (solid)	c	1466 $Jkg^{-1}K^{-1}$
Specific heat capacity (gas)	c_g	1960 $Jkg^{-1}K^{-1}$
Density	ρ	1200 kgm^{-3}
Activation temperature	T_A	17072.2 K
Natural log of pre-exponential factor	J	20.76 $\ln(s^{-1})$
Heat of reaction (gasification)	H_g	0.84 $MJkg^{-1}$

Table 1. Model parameter values.

The in-depth length scale for radiation, thermal conductivity, critical ignition mass flux and density were taken in-line with other values used in the literature [5], [14]. The convection heat transfer coefficient was taken as a representative value from a recent detailed experimental investigation [15]. The flame heat flux was taken from other studies [9], [10] and the heat of the gasification reaction was calculated from average bond energies [16]. The specific heat capacity of the solid was taken as a

representative value for PMMA and the specific heat capacity of the gas as a representative value for MMA (both obtained from WWW-based data tables).

The Arrhenius parameters A and T_A for the reaction rate are obtained from constant heating rate thermogravimetric (TG) experiments for standard PMMA samples in nitrogen, previously published in an earlier study [17]. It was felt important to estimate these parameters from an experiment in an inert atmosphere since the oxygen concentration at the exposed surface is likely to be significantly below normal atmospheric levels due to out-gassing of MMA. There is a problem with using TG data at standard heating rates such as 10 - 50 K/min in that in practice, the heating rates at the exposed surface of the sample will greatly exceed these values. For example, at 50 KWm^{-2}, the ignition time of black PMMA is ~30 s, indicating a heating rate at the exposed surface of ~600 K/min. At 100 kWm^{-2}, the corresponding heating rate is ~1800 K/min. Without specialised equipment it is impossible to investigate thermal degradation at such high heating rates and so data from our analyser's maximum heating rate of 50 K/min was used. Naturally, if one were concerned with a detailed examination of the kinetic mechanism then this heating rate would be too high. However, in this application heating rates are so high that it is likely that many of the individual nuances of the degradation mechanism will be smeared together. This perhaps may account for the reason why more detailed kinetic mechanisms do not explain the observed ignition trend at high heat flux as noted by Bal & Rein [5].

In order to obtain estimates of the Arrhenius parameters, model fits were compared to both experimental mass loss and mass derivative curves. Residuals for the fits to each curve were calculated and the sum of residuals was minimised in order to obtain the best parameter estimates. The resulting best fits are shown in Figure 4.

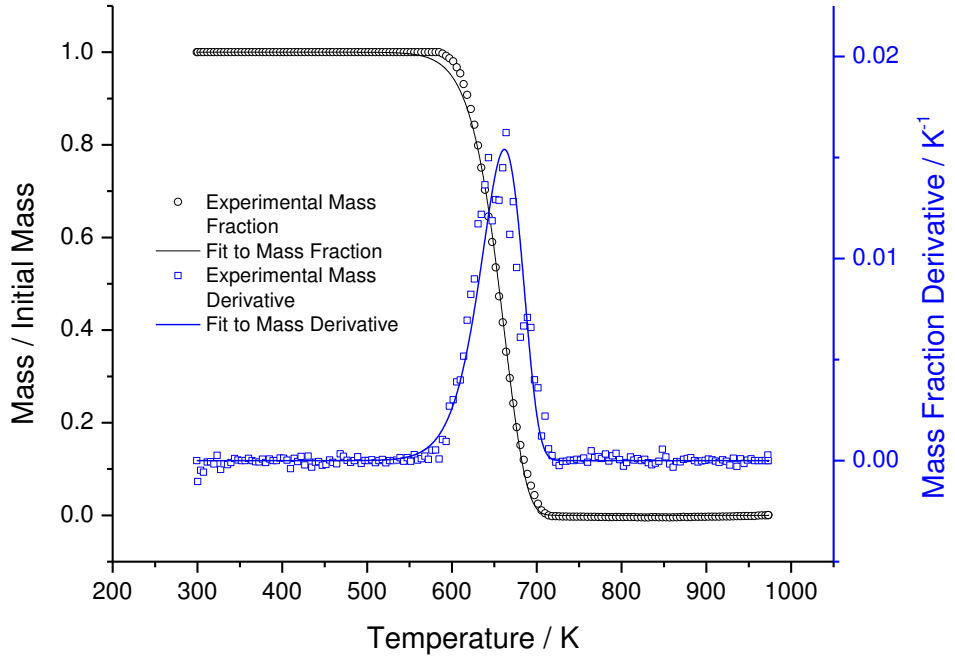

Figure 4. Constant heating rate TG data and optimal fits for PMMA at 50 K/min.

The absorptivity α_R and absorption coefficient κ were estimated by comparing model predictions for mass flux to experimental cone calorimeter results at an external heat flux of 50 kWm^{-2}, using a PMMA sample of initial thickness 12 mm. Figure 5 shows a contour plot of the residual, defined by

$$\text{Residual} = \left\{ \frac{1}{t_{stop}} \int_0^{t_{stop}} \left(\dot{m}''_{exp} - \dot{m}''_{model} \right)^2 dt \right\}^{1/2}, \qquad (20)$$

where $\dot{m}''_{exp}$ is the experimental mass flux from the cone calorimeter and $\dot{m}''_{model}$ is the predicted mass flux from the model.

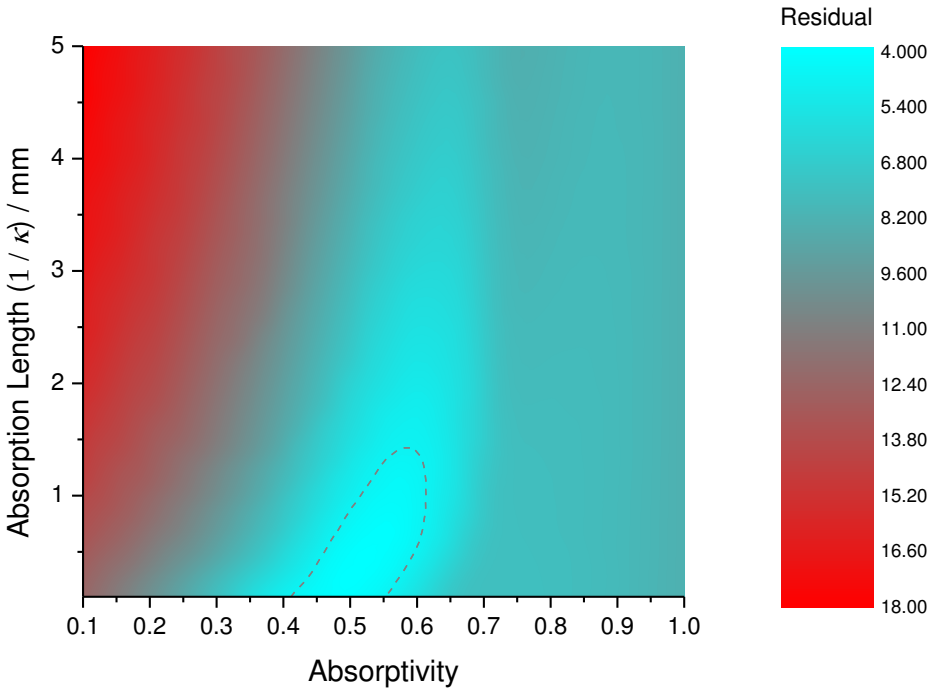

Figure 5. Contour plot of mass flux residual.

It is apparent from Figure 5 that the residual has an approximately flat basin (shown by the dashed curve) in the neighbourhood of the minimum. This unfortunately means that there is no clearly defined optimum and any values within the dashed region will produce good fits to the experimental data. Therefore, broadly in line with other observations [4], [5] it was decided to take $1/\kappa$ as 1 mm and seek the optimum α_{R} that minimised the residual. This process gives the best value of α_{R} as 0.56, as Figure 6 confirms. Figure 7 shows the optimum fit together with the experimental data for comparison.

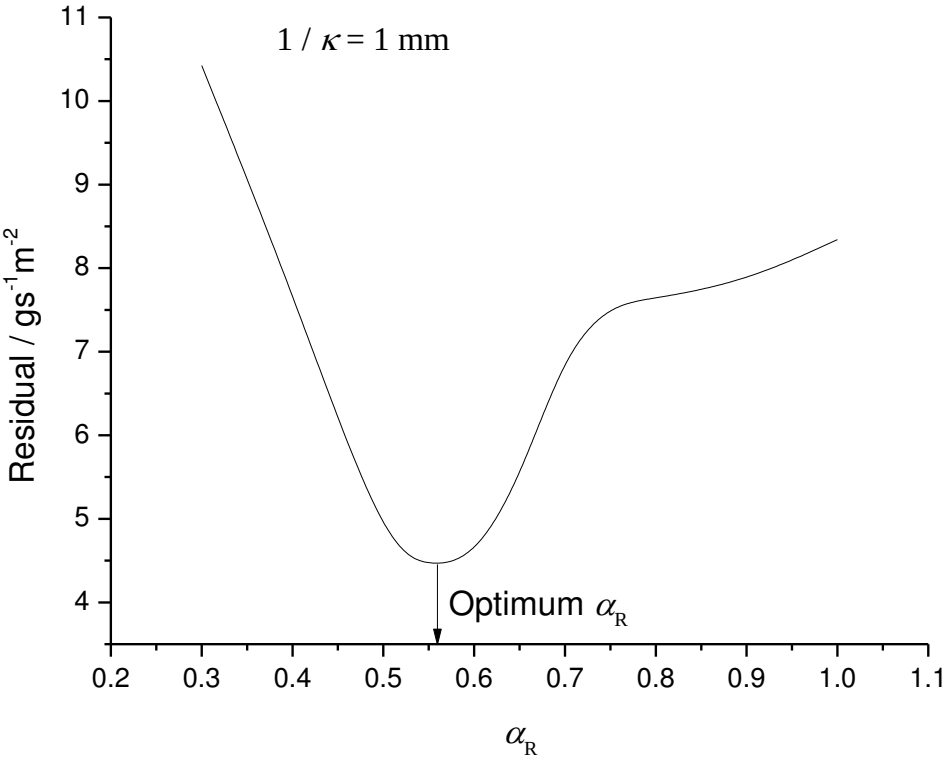

Figure 6. Optimum α_R for $1 / \kappa = 1$ mm.

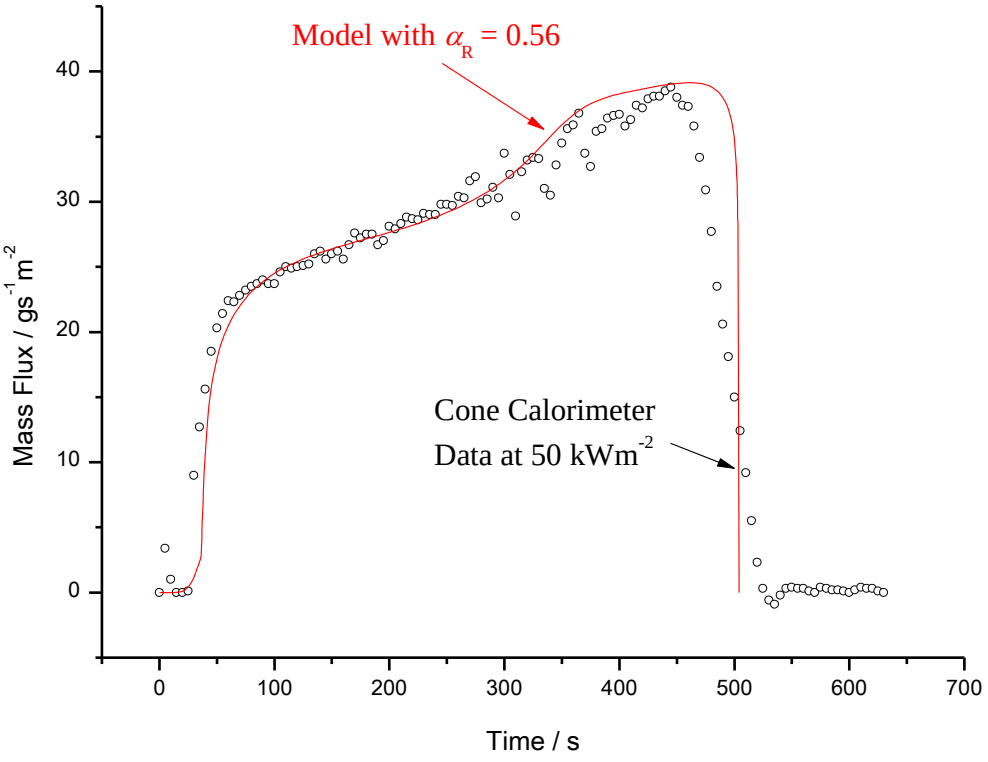

Figure 7. Comparison of model with cone calorimeter results for standard parameter values shown in Table 1.

Unfortunately there is a lack of information to quantify the gas-phase absorption parameter. Kashiwagi's earlier work [1] suggests that there was significant gas-phase absorption in his experiments. However, the apparatus used in his work and the spectral characteristics of the heat source are significantly different to an oxygen consumption calorimeter and the discussion in §3.2 suggests that there is every reason to suppose that the gas phase absorption parameter is sensitively dependent on experimental apparatus. Given that ignition occurs at a relatively low mass flux, in a well-ventilated experiment such as a cone calorimeter it is reasonable to suppose that gas-phase absorption plays little part in ignition. However, in the quasi-steady region where mass flux is significantly higher than at ignition, it is possible that gas-phase absorption is important.

5. Results

Beaulieu [2], [3], presented empirical ignition results that are representative of a broader super-set discussed by Bal & Rein [5]. Beaulieu's results were obtained using 25 mm thick specimens in the AFM apparatus where an infra-red lamp is used as the heat source. Neither Beaulieu or Bal & Rein make mention of the earlier work of Kashiwagi [1], where a CO_2 laser was the primary heat source used and delivered similar levels of heat flux at the exposed surface.

Figure 8 shows results from the model with the parameter set given in Table 1 with the experimental data of Beaulieu [2], [3], Kashiwagi [1] and the coated PMMA data of Jiang et al. [4]. Also shown in the figure are model results obtained with slightly different values for κ and α_R, corresponding to the upper region of the dashed area shown in Figure 5. As suggested above, it was found that the gas-phase absorption parameter μ had little discernible effect on ignition behaviour for values in the range 0 – 10 m^2skg^{-1} and so no results are explicitly included in Figure 8.

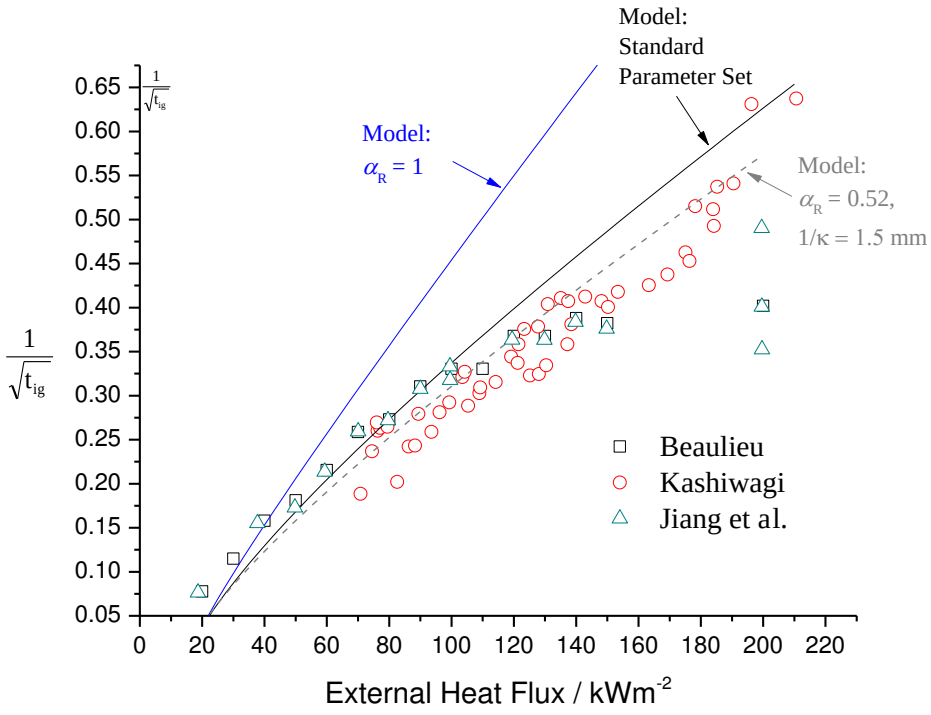

Figure 8. Comparison between model and experimental data for ignition time (in seconds).

The obvious point to note is the model confirms that in-depth absorption plays an important role in ignition at high heat flux. Also, the scaling given by Eqn. (11) is preserved, i.e. $1/\sqrt{t_{ig}}$ reduces approximately in direct proportion to α_R at high heat flux.

Naturally, an optimum choice for α_R could be found by computing the best fit of model predictions directly with the experimental data in Figure 8. However, the author felt that a stronger case for the validity of the model could be promoted if a value for α_R was found at a single heat flux and then used for model predictions across the heat flux spectrum.

The graph in Figure 9 shows the effect of varying the gas-phase absorption parameter without ignition when the external heat flux is set to 100 kWm^{-2}. The dependent axis corresponds to the ratio of heat flux at the sample surface to $\dot{q}''_{ext}$, i.e. 1 – attenuation, and the dependent axis is time. The graph in Figure 10 shows the same heat flux ratio, but with μ fixed at 5.0 m^2skg^{-1} for the three heat fluxes that Kashiwagi used in his experiments [1]. Although the magnitude of attenuation at this value of μ is much less than Kashiwagi reported, the qualitative behaviour is strikingly similar.

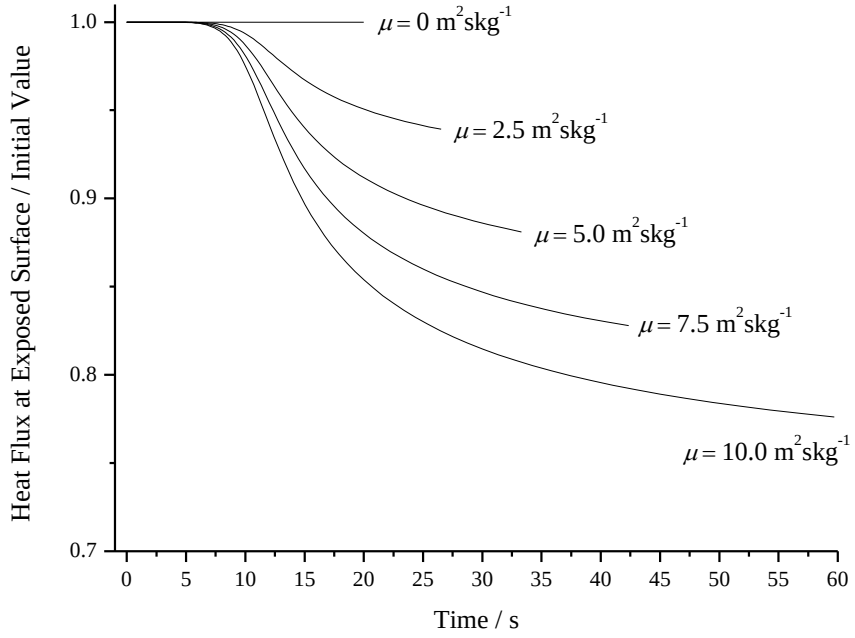

Figure 9. Effect of gas-phase absorption parameter μ on attenuation

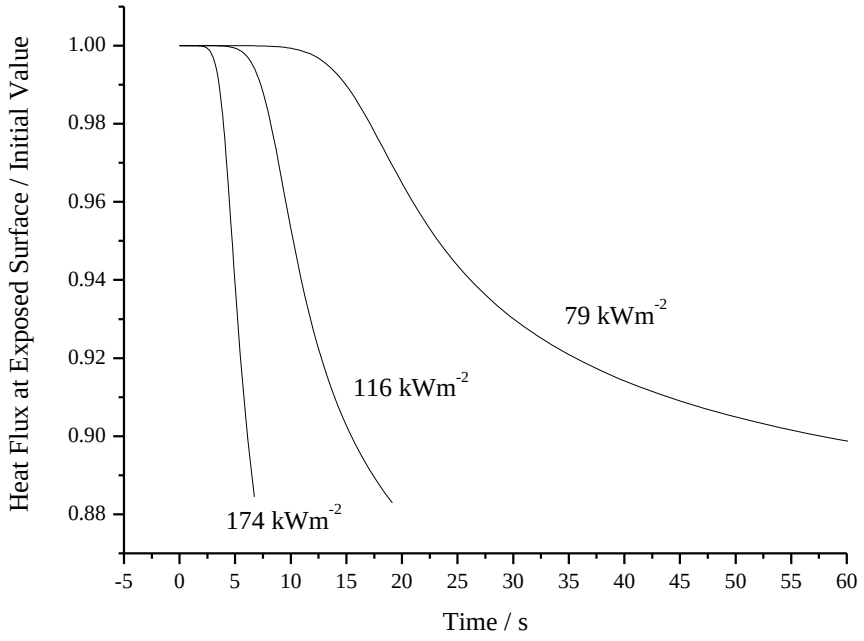

Figure 10. Effect of external heat flux on attenuation.

Beaulieu [3] reported interesting behaviour for the steady-state sample mass flux at high external heat flux. As heat flux increased, her measurements showed a nonlinear

variation in steady mass flux with external heat flux at odds with the prediction from simple ablation theory that steady mass flux is proportional to the ratio of external heat flux to heat of gasification. Results from the model proposed here suggest that this variation can be explained, at least in part, by gas-phase absorption of radiation. The graph in Figure 11 shows Beaulieu's data for steady mass flux together with model predictions for various values of the gas-phase absorption parameter. We note that for external heat fluxes below 70 kWm^{-2}, the empirical values agree with model predictions for zero gas-phase absorption ($\mu = 0$). However for heat fluxes above this value agreement only improves when μ is increased. Analysis of the total sum-of-squares residual[3] (Figure 12) indicates that $\mu \sim 6.1 m^2 skg^{-1}$ provides the best overall fit.

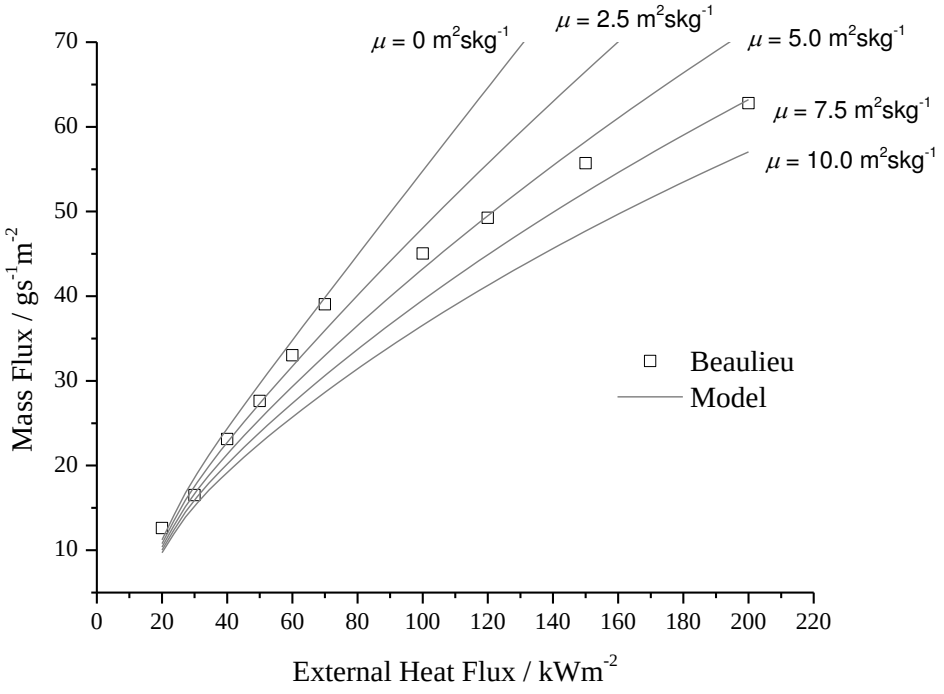

Figure 11. Comparison between model results for various values of the gas-phase absorption parameter μ and Beaulieu's AFM data for mass flux [3].

[3] Defined analagously to Eqn. (20).

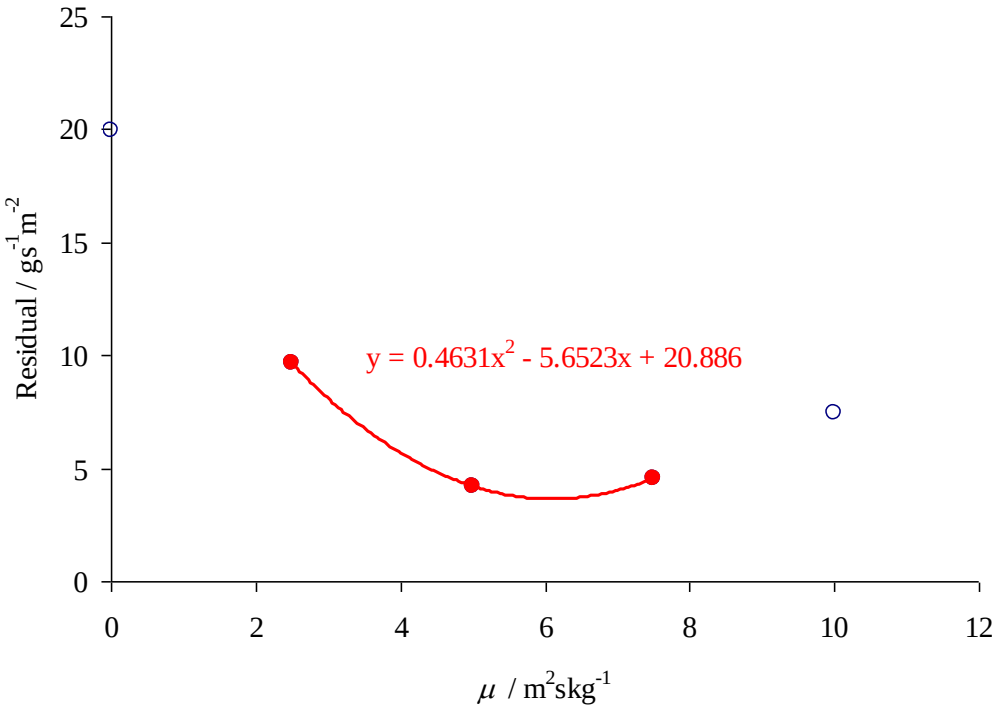

Figure 12. Goodness of fit of numerical results to observed mass flux.

Of course, a major assumption in the model is that flame heat flux is invariant to changes in external heat flux. In all likelihood this assumption is faulty, but is probably not responsible for the observed behaviour for the following reason. As external heat flux increases mass flux will also increase, which implies that if combustion conditions remain broadly similar in the flame, then more heat should be released. In other words, if anything we should expect the flame heat flux to increase with external heat flux, which would have the effect of increasing mass flux above the expected value. In reality, as Figure 11 shows, the observed mass flux increases with external heat flux more slowly than expected.

It is also unlikely that the kinetic mechanism can explain the deviation as increasing external heat flux serves only to increase the temperature in the degrading solid. Consequently since most degradation reaction rates are known to increase with temperature, this is also unlikely to be the cause.

6. Discussion and Conclusion

The analysis above lends further support to the suggestion that in-depth absorption of radiation plays an increasingly important role in the ignition behaviour of PMMA as external heat flux increases. The effect of in-depth absorption is to extend the ignition delay time above what might be expected when it is ignored. Furthermore, it is also likely that the quasi-steady mass flux (or burning rate) is strongly influenced by absorption of external radiation by the pyrolyzate in the gas phase above the sample at high external heat flux. Experimental results from external heating by CO_2 laser confirm that absorption by the pyrolyzate is significant (although there are no simultaneous measurements of mass flux). Experiments using cone calorimeter type apparatus show that burning rate is lower than expected at high heat flux (although there are no simultaneous measurements of gas-phase attenuation). A model of gas-phase absorption was developed that predicted radiation attenuation to vary exponentially with mass flux. Results from the model suggest that gas phase absorption has little effect on ignition, but supports the hypothesis that there may be a significant effect on mass flux. Unfortunately it is not yet possible to make a firm statement about this effect due to the lack of experimental data correlating attenuation with mass flux.

A further complication that is difficult to address fully is the amount of energy that is actually absorbed by a solid or gas from a radiant heat source. The quantity of energy absorbed is strongly dictated by the wavelength of the incident radiation. The solid or gas absorbs radiation mainly in discrete bands of the infra-red spectrum, implying that the absorption coefficients will depend on wavelength. In other words, if the wavelength of the incident radiation changes, then the relative amount of energy absorbed is likely to change. It is for this reason that Kashiwagi chose to use a CO_2 laser for his study [1] - it is, to a good degree of approximation, essentially monochromatic. The emmision spectra of other heat sources used in the ignition studies cited in this paper will be different, and may well vary with heat flux, and this might play a significant part in some of the discrepancies noted above in empirical observations. In particular, the observation reported by Beaulieu [2] that there

appeared to be little gas-phase absorption of radiation for propene is at odds with Kashiwagi's observations of attenuation by PMMA pyrolyzate using the CO_2 laser and wavelength dependence of absorption could well be at the heart of this inconsistency. The model used in the analysis above makes no allowance for wavelength dependent effects and it may be for this reason that the agreement between numerical results and ignition delay time is better for the monochromatic CO_2 laser source than the heat source used in the AFM apparatus used by Beaulieu.

Another consideration to keep in mind when weighing the results reported here is the relative importance of the thermal degradation mechanism of the solid fuel. PMMA is typically chosen for study because it undergoes depolymerisation on heating. As soon as radical fragments form by random cleavage, they rapidly unzip to produce MMA monomer. If the unzipping process is much faster than the random cleavage process (which is typically the case) then the rate-determining step for monomer production will be determined by the rate of random cleavage. A more detailed study of modelling the degradation mechanism of PMMA was undertaken by the author using population balance methods [17]. In that work the author was able to demonstrate that for an initial population of molecules with high degree of polymerisation, when unzipping is much faster than initiation by random scission, it is possible to show that the production rate of monomer is well modelled by a process that is essentially similar to a one-step Arrhenius process. The model above uses a simple one-step degradation process, which is a gross oversimplification of the true mechanism, but at high heating rates may not be too limiting for PMMA. The validity of this simplification for other polymers is highly dubious however.

References

[1] Kashiwagi T. Experimental observation of radiative ignition mechanisms. Combustion & Flame 1979; 34: 231-244.

[2] Beaulieu P. A. Flammability Characteristics at Heat Flux Levels up to 200 kW/m^2 and the Effect of Oxygen on Flame Heat Flux, PhD Dissertation, Worcester Polytechnic Institute, 2005. <http://www.wpi.edu/Pubs/ETD/Available/etd-121905-082146/unrestricted/beaulieu.pdf> (accessed 3rd July 2012).

[3] Beaulieu P. A. , Dembsey N. Flammability characteristics at applied heat flux levels up to 200 kW/m^2. Fire & Materials 2008; 32: 61–86.

[4] Fenghui Jiang, de Ris J. L. & Khan M. M. Absorption of thermal energy in PMMA by in-depth radiation. Fire Safety Journal 2009; 44: 106-112.

[5] Bal N., Rein G. Numerical investigation of the ignition delay time of a translucent solid at high radiant heat fluxes. Combustion & Flame 2011; 158: 1109-1116.

[6] Staggs J. E. J. Thermal degradation of solids using single-step first-order kinetics. Fire Safety Journal 1999; 32: 17-34.

[7] Kindelan M. & Williams F. A. Theory for endothermic gasification of a solid by a constant energy flux. Combustion Science and Technology 1975; 10: 1-19.

[8] Tewarson A. & Pion R. F. Flammability of plastics I- Burning intensity. Combustion & Flame 1977; 26: 85-103.

[9] B. T. Rhodes & J. G. Quintiere. Burning rate and flame heat flux for PMMA in a cone calorimeter. Fire Safety Journal 1996; 26: 221-240.

[10] Hopkins Jr. & J. G. Quintiere. Material fire properties and predictions for thermoplastics. Fire Safety Journal 1996; 26: 241-268.

[11] Staggs J. E. J. A Theory For Quasi-Steady Single-Step Thermal Degradation of Polymers. Fire and Materials 1998; 22: 109-118.

[12] Staggs J. E. J. A theoretical investigation into modelling thermal degradation of solids incorporating finite-rate kinetics. Comb. Sci. & Tech. 1997; 123: 261

[13] Delichatsios M. A., Zhang J. An alternative way for the ignition times for solids with radiation absorption in-depth by simple asymptotic solutions. Fire & Materials 2012; 36: 41–47.

[14] Staggs J. E. J., Nelson M. I. A critical mass flux model for the flammability of thermoplastics. Combustion Theory & Modelling 2001; 5: 399-427.

[15] Staggs J. E. J. A Reappraisal of Convection Heat Transfer in the Cone Calorimeter. Fire Safety Journal 2011; 46: 125-131.

[16] Staggs J. E. J. The heat of gasification of polymers. Fire Safety Journal 2004; 39: 711-720.

[17] Staggs J. E. J. Population balance models for the thermal degradation of PMMA. Polymer 2007; 48: 3868-3876.